#4690

Multi-sample automation of the CLARITY technology for the processing of 3D volumes of tissue

Sharla L. White, Yi Chen, Qi Shen, Laurie J. Goodman
ClearLight Biotechnologies, LLC 428 Oakmead Parkway, Sunnyvale, CA 94085

ABSTRACT

The current technologies utilized for preclinical and clinical drug development in cancer is largely dependent upon the 2-dimensional (2D) analysis of thin Formalin-Fixed Paraffin-Embedded (FFPE) tissue sections (5-10 µm). However, the importance of understanding cellular phenotypic information combined with three-dimensional (3D) spatial analysis of tissues has recently evolved. In recent years, several clearing techniques, such as CLARITY, have been developed and modified as a means to image and evaluate these volumetric tissues. Most of these techniques have employed chemical approaches to improve tissue clearing, while inadvertently affecting the tissue integrity on a macroscopic or microscopic level. Our previous work with CLARITY has demonstrated how the tissue-hydrogel matrix (HM) is able to maintain its structural integrity overall. Yet, some of the most noted caveats to employing this technique has been the lengthy processing times, and the lack of robust 3D spatial analysis software. We sought to address these issues through the development of an automated clearing and staining platform for CLARITY processed tissues with a proprietary 3D image analysis employing artificial intelligence and machine learning techniques. All experiments were performed with the CLARITY technique using HM-embedded tissues that were cleared with a SDS/borate clearing buffer. Evaluation of the clearing module was assessed using a passive staining (diffusion-based) approach before sample imaging. The effectiveness of the staining module was assessed using passively cleared tissues that were "actively" stained using the developed respective module, followed by standard imaging. The imaging data was then uploaded into our proprietary 3D software for segmentation, classification, and quantitative spatial analysis. We were able to demonstrate successful clearing and staining in both normal and cancerous tissue samples in a total time of less than one day. Consistent results are obtained for both fresh and formalin-fixed tissues. This was a significant reduction in the time associated with the standard passive clearing and staining procedure. In short, the development of our end-to-end multi-sample clearing and staining platform not only removes the laborious sectioning and sample registration for sample reconstruction, but also maintains the benefits of multiple interrogation of a single sample. Although volumetric clearing and 3D analysis are still in their infancy from a technology perspective, one tissue sample using these novel approaches provides as much volumetric information as 200 FFPE sections, while also maintaining key spatial information.

1. THE CLARITY TECHNOLOGY WORKFLOW

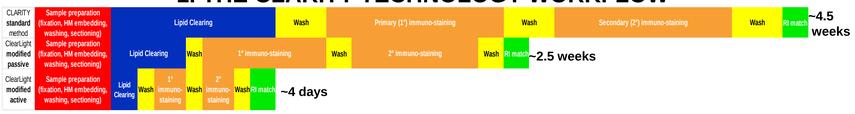

Figure 1. We have sought to optimize and modify various CLARITY parameters that have improved both the clearing and staining of thick HM-embedded tissues. Additionally, preliminary data suggests if both our active clearing and active staining modules were employed, clearing and staining could be complete in ~24 hours.

2. ACTIVE CLEARING MODULE

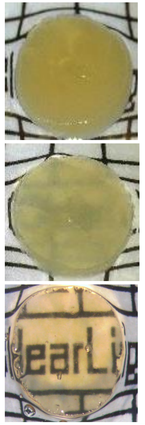

Figure 2. A normal mouse kidney (5 x 1 mm) biopsy punch sample before active clearing (Top), after 30 mins of active clearing (center), and RI matched prior to confocal imaging (bottom).

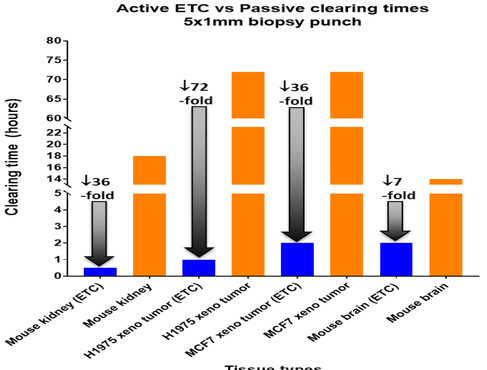

Figure 3. Our active clearing module significantly decreased the clearing time for various 5 x 1 mm biopsy punch tissue samples, including normal mouse tissues and cell line xenograft tumors.

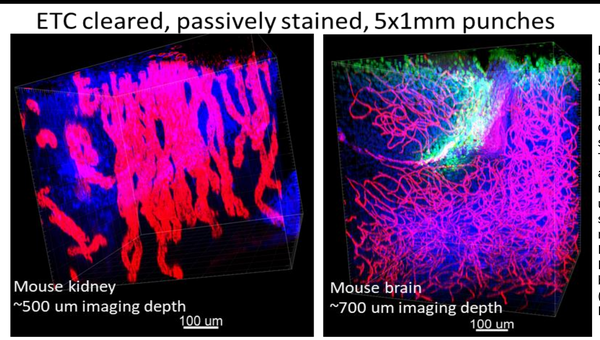

Figure 4. A 3D image of passive macromolecule staining of ETC cleared normal mouse kidney and mouse brain demonstrate the retention of cellular and subcellular structures at 20x magnification. The samples were imaged on a Leica SP8 confocal microscope and visualized using Bitplane Imaris 9.2.1 software. Left image: Normal mouse kidney, Tomato Lectin – DyLight 594 (red), DAPI (blue). Right image: Normal mouse brain, Histone H3 – AF647 (green), Tomato Lectin – DyLight 594 (red), DAPI (blue).

3. ACTIVE STAINING MODULE

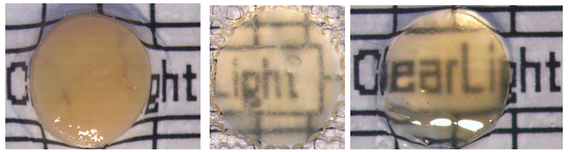

Figure 5. A normal mouse kidney (5 x 1 mm) biopsy punch sample before passive clearing (left), after passive clearing (center), and actively stained/RI matched (right). The actively stained sample was photographed after confocal imaging was complete.

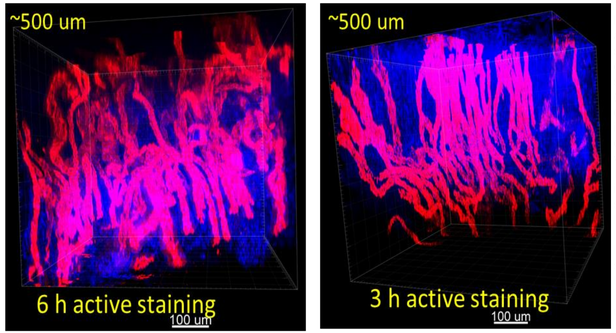

Figure 6. A 3D image of an active macromolecule staining with a passively cleared normal mouse kidney stained for two different times (~500 microns of staining detected). The samples were imaged on a Leica SP8 confocal microscope and visualized using Bitplane Imaris 9.2.1 software. Left image: Normal mouse kidney stained for 6 hours, Tomato Lectin – DyLight 594 (red), DAPI (blue). Right image: Normal mouse kidney stained for 3 hours, Tomato Lectin – DyLight 594 (red), DAPI (blue). 20x magnification.

5. SUMMARY

- Our active clearing and staining modules resulted in a significant reduction in the time associated with the standard passive clearing and staining procedure.
- Technologically, volumetric clearing and 3D analysis are still in their infancy; however, our automated platform development and proprietary software demonstrate great promise.
- The development of our end-to-end multi-sample clearing and staining platform, with individualized sample chambers, not only removes the laborious sectioning and tissue cross-contamination, but also the need of sample registration for 3D reconstruction.

4. 3D SOFTWARE ANALYSIS WORKFLOW

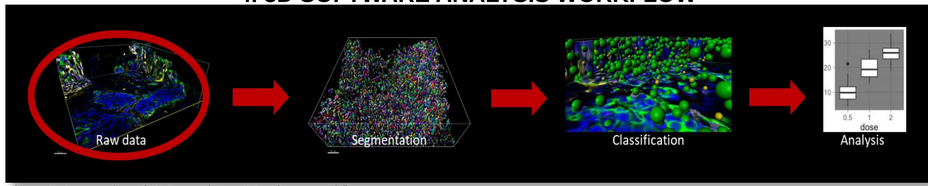

Figure 7. An overview of CLB proprietary 3D software workflow.

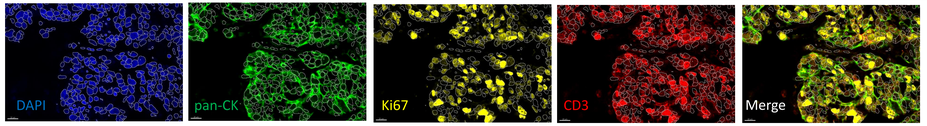

Figure 8. 2D optical section of a HM-embedded breast cancer tissue demonstrating an overlay of cell segmentation with each biomarker using a HM embedded clinical breast cancer needle core biopsy previously described (Chen Y., et al., Scientific Reports, 2019 - accepted). The samples were imaged on a Leica SP8 confocal microscope and using Bitplane Imaris 9.2.1 software.

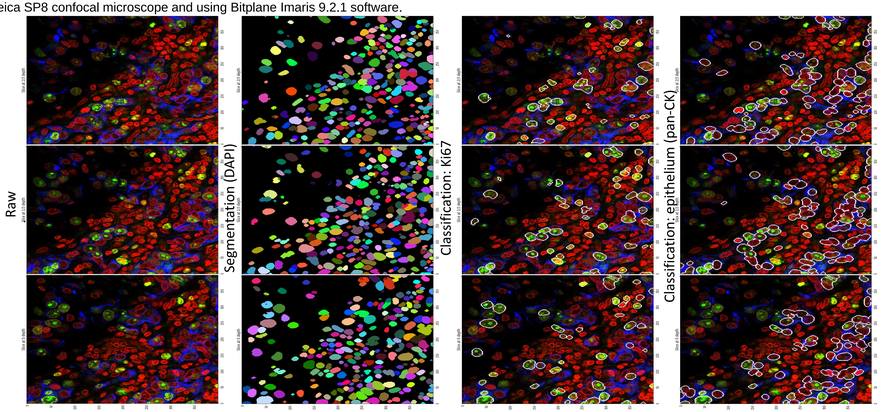

Figure 9. An analyzed 2D representation of cell segmentation and classification for a HM embedded clinical breast cancer needle core biopsy tissue performed using our proprietary software. The visualization of cell segmentation and classification is shown using Imaris 9.2.1 software.

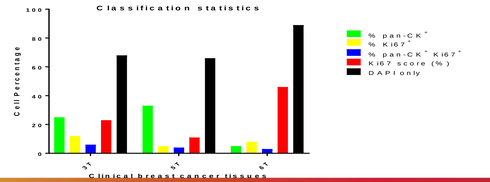

Figure 10. Preliminary quantitative analysis performed on HM-embedded clinical breast cancer needle core biopsy tissues, (Chen Y., et al., Scientific Reports, 2019 - accepted) following cell segmentation and classification. Only one volumetric field of view was analyzed per sample on the 3D software. The Ki67 score was calculated by 'the number of Ki67 positive epithelial cells / the total number of epithelial cells' (at least 9000 cells were counted per view). Segmented cells lacking pan-CK or Ki67 expression were noted as DAPI only cells.